Original Article | Gastrointestinal Imaging

eISSN 2005-8330
https://doi.org/10.3348/kjr.2021.0055
Korean J Radiol 2021;22(11):1797-1808

Korean Journal of Radiology
KJR

Volumetric CT Texture Analysis of Intrahepatic Mass-Forming Cholangiocarcinoma for the Prediction of Postoperative Outcomes: Fully Automatic Tumor Segmentation Versus Semi-Automatic Segmentation

Sungeun Park[1, 2], Jeong Min Lee[1, 3, 4], Junghoan Park[1], Jihyuk Lee[1], Jae Seok Bae[1], Jae Hyun Kim[1, 3], Ijin Joo[1, 3]

[1]Department of Radiology, Seoul National University Hospital, Seoul, Korea; [2]Department of Radiology, Konkuk University Medical Center, Seoul, Korea; [3]Department of Radiology, Seoul National University College of Medicine, Seoul, Korea; [4]Institute of Radiation Medicine, Seoul National University Medical Research Center, Seoul, Korea

Objective: To determine whether volumetric CT texture analysis (CTTA) using fully automatic tumor segmentation can help predict recurrence-free survival (RFS) in patients with intrahepatic mass-forming cholangiocarcinomas (IMCCs) after surgical resection.

Materials and Methods: This retrospective study analyzed the preoperative CT scans of 89 patients with IMCCs (64 male; 25 female; mean age, 62.1 years; range, 38–78 years) who underwent surgical resection between January 2005 and December 2016. Volumetric CTTA of IMCCs was performed in late arterial phase images using both fully automatic and semi-automatic liver tumor segmentation techniques. The time spent on segmentation and texture analysis was compared, and the first-order and second-order texture parameters and shape features were extracted. The reliability of CTTA parameters between the techniques was evaluated using intraclass correlation coefficients (ICCs). Intra- and interobserver reproducibility of volumetric CTTAs were also obtained using ICCs. Cox proportional hazard regression were used to predict RFS using CTTA parameters and clinicopathological parameters.

Results: The time spent on fully automatic tumor segmentation and CTTA was significantly shorter than that for semi-automatic segmentation: mean ± standard deviation of 1 minutes 37 seconds ± 50 seconds vs. 10 minutes 48 seconds ± 13 minutes 44 seconds ($p < 0.001$). ICCs of the texture features between the two techniques ranged from 0.215 to 0.980. ICCs for the intraobserver and interobserver reproducibility using fully automatic segmentation were 0.601–0.997 and 0.177–0.984, respectively. Multivariable analysis identified lower first-order mean (hazard ratio [HR], 0.982; $p = 0.010$), larger pathologic tumor size (HR, 1.171; $p < 0.001$), and positive lymph node involvement (HR, 2.193; $p = 0.014$) as significant parameters for shorter RFS using fully automatic segmentation.

Conclusion: Volumetric CTTA parameters obtained using fully automatic segmentation could be utilized as prognostic markers in patients with IMCC, with comparable reproducibility in significantly less time compared with semi-automatic segmentation.

Keywords: *Adults (Human); Liver; CT-quantitative; Computer applications-texture analysis; Tumor response*

INTRODUCTION

Intrahepatic cholangiocarcinoma is the second most common primary liver cancer following hepatocellular carcinoma [1], and its incidence, albeit relatively rare, has been increasing worldwide over the past two decades

Received: January 28, 2021 **Revised:** April 8, 2021 **Accepted:** April 27, 2021
Corresponding author: Jeong Min Lee, MD, Department of Radiology and Institute of Radiation Medicine, Seoul National University College of Medicine, Seoul National University Hospital, 101 Daehak-ro, Jongno-gu, Seoul 03080, Korea.
• E-mail: jmlshy2000@gmail.com

[2,3]. Currently, surgical resection is the only potentially curative treatment option for patients with intrahepatic cholangiocarcinoma [4,5]; however, even after curative surgery, clinical outcomes remain poor, with a 5-year survival rate of only 20–35% [4]. Previous studies [6-8] have demonstrated large tumor size, lymph node metastasis, and multiplicity as risk factors for recurrence after resection. Further attempts to predict the prognosis of intrahepatic mass-forming cholangiocarcinoma (IMCC) through imaging findings revealed that arterial and delayed enhancement can be utilized as potential prognostic markers of IMCC [9-12]. However, these imaging features can be considered to be rather subjective; thus, quantitative prognostic imaging markers would be of great clinical value, given the poor prognosis and lack of well-established treatment options in patients with IMCCs.

In recent years, radiomics and texture analysis have become an important area of research in oncology as clinical decision support tools [13-15]. Texture analysis is a novel non-invasive technique that quantifies the spatial pattern of pixel intensities on cross-sectional imaging to evaluate the heterogeneity of tumors [13,15,16], which is known to be a relevant factor in tumor prognosis [17-21]. Moreover, studies have shown that tumors with high intratumoral heterogeneity, representing higher spatial variation in cellularity, angiogenesis, tumor matrix, and areas of necrosis, have a poorer prognosis [22,23]. Previous studies have reported that a new nomogram using texture parameters extracted from manual segmentation of the arterial phase of MRI was able to predict the early recurrence of intrahepatic cholangiocarcinoma [24]. Despite the growing clinical interest in radiomics, several technical challenges hinder its further adoption, including a lack of standardization in extracting radiomics features and reproducibility [25,26]. For instance, the selection of the region of interest (ROI) can greatly influence textural index estimations, as it largely depends on the segmented area or volume [13,21]. This would be particularly critical in IMCC, as these tumors generally have indistinct borders. In this regard, Parmar et al. [27] reported that semi-automatic segmentation may improve the robustness of texture analysis features compared with manual segmentation in non-small-cell lung cancers on CT. Since then, many attempts to apply automatic segmentation for liver tumors have yielded similar performance for radiologists [28,29]. However, until now, no CT texture analysis (CTTA) study has been performed for cholangiocarcinoma using an automatic segmentation tool to predict its prognosis.

Therefore, this study aimed to determine whether volumetric CTTA using a fully automatic segmentation technique is useful in predicting recurrence-free survival (RFS) in patients with IMCC in comparison with semi-automatic volumetric segmentation analysis.

MATERIALS AND METHODS

Patients

The Institutional Review Board of Seoul National University Hospital approved this retrospective study, and the requirement for informed consent was waived (IRB No. 1703-015-836). Data for our clinical study group was obtained from the electronic medical records of our tertiary hospital and consisted of 89 patients (64 male and 25 female; mean age, 62.1 years; range, 38–78 years) who were pathologically diagnosed with IMCCs after surgery between January 2005 and December 2016. The inclusion criteria were as follows: 1) pathologically confirmed IMCC after curative-intent surgery (i.e., R0 resection achieved), 2) availability of preoperative contrast-enhanced pancreatobiliary or liver protocol CT images including the late arterial phase, 3) CT images reconstructed using filtered back projection (FBP) at 120 kVp, 4) interval between preoperative CT scans and surgery of less than 8 weeks, and 5) follow-up longer than at least 6 months after surgery.

The exclusion criteria were as follows: 1) patients with distant metastasis at initial workup (n = 5), 2) other concurrent malignancy or history of other malignancies (n = 35), 3) those who underwent treatment for IMCC such as radiofrequency ablation or transcatheter arterial chemoembolization before surgery (n = 10), and 4) technical errors during uploading CT images (n = 2). A detailed description of the inclusion and exclusion of the study patients is summarized in Figure 1.

Clinical and Pathologic Parameters

The pathologic data of the surgical specimens were retrieved from the pathologic reports registered in the electronic medical records of our hospital, including gross type, resection margin, size, histologic grade, number of tumors, presence or absence of an extrahepatic extension, vascular invasion or regional lymph node metastasis, and underlying hepatitis (including liver cirrhosis). Other demographic and clinical data were also collected, including age; sex; laboratory findings such as carbohydrate

https://doi.org/10.3348/kjr.2021.0055

Korean Journal of Radiology
KJR

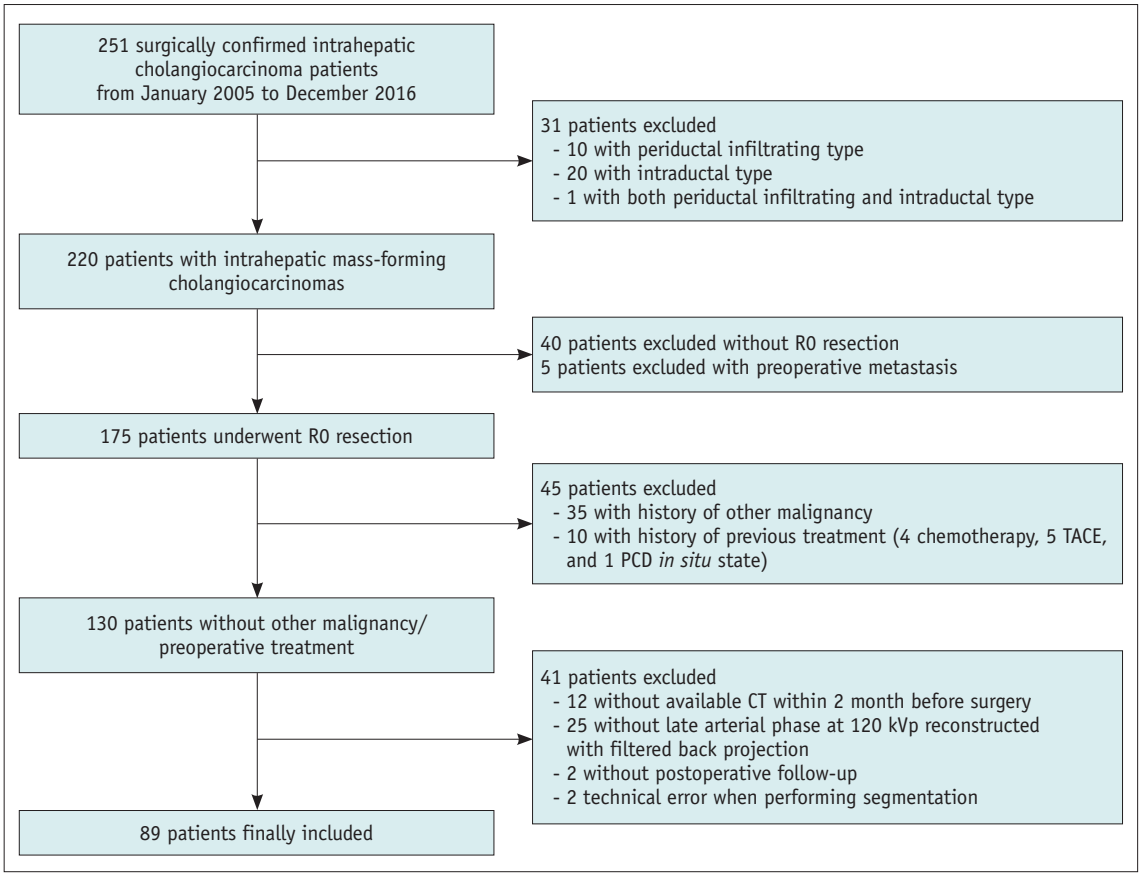

Fig. 1. Flowchart of the inclusion and exclusion of study patients. PCD = percutaneous catheter drainage, TACE = transcatheter arterial chemoembolization

antigen 19-9, cancer embryonic antigen (CEA), aspartate transaminase, alanine aminotransferase, total bilirubin, and albumin; and whether preoperative treatment for IMCC was performed.

Follow-Up

All patients were followed up until tumor recurrence (either regional or distant) or the final outpatient visit until December 2019. Surveillance for tumor recurrence was performed at least once every 6 months in an outpatient setting using imaging modalities, including ultrasound, CT, or MRI. Tumor recurrence time was defined as the time at which the tumor was detected in at least one of the imaging modalities listed above.

CT Acquisition

A variety of CT scanners were used in our study owing to its retrospective design and relatively low incidence of IMCCs. All 89 preoperative CT examinations were performed using a multidetector CT system with four (n = 4), eight (n = 8), 16 (n = 24), 32 (n = 3), 64 (n = 45), or 320 (n = 5) slices. CT parameters were as follows: tube voltage, 120 kVp; tube current, 99–187 mAs; rotation time, 0.5 seconds; pitch, 1.0–1.5; slice thickness, 2.5–3 mm; and reconstruction interval, 2–2.5 mm. After administration of 1.6 mL/kg of nonionic contrast material at a rate of 3.0–5.0 mL/s using a power injector, late arterial phase helical CT scans were obtained according to the bodyweight of the patient. For late arterial phase scanning, a 17–19 seconds delay was used after the maximal Hounsfield unit (HU) of the descending thoracic aorta reached 100 HU using bolus tracking. All images were reconstructed using the FBP algorithm.

Only CT scans performed within 8 weeks before surgery were included. If more than one late arterial phase CT examination was available, the CT nearest to the operation day was selected.

Texture Analysis

All late arterial phase CT images were retrieved from our picture archiving and communication system and loaded into a commercially available texture analysis software

 https://doi.org/10.3348/kjr.2021.0055

program (Syngo.via Frontier, RADIOMCIS prototype, Siemens Healthineers) for further texture analysis. Texture analysis was performed by one radiologist (5 years of abdominal CT experience) using an automatic liver lesion segmentation tool (Fig. 2) provided in the prototype CT Multiparameter Analysis software (Syngo.via Frontier, RADIOMCIS prototype, Siemens Healthineers), which was performed by a user-defined stroke for the long diameter of each lesion (the largest lesion, if multiple tumors were present). The automatic lesion segmentation algorithm used in our study has been described in a previous study [30,31]. In brief, it consists of three parts: region growing, ray casting, ellipsoid approximation, and convex hull.

The first-order texture analysis with seven parameters (mean, variance, energy, entropy, skewness, kurtosis, and uniformity); second-order texture analysis (Gray-Level Co-occurrence Matrix [GLCM]) with seven features (inverse difference moment, contrast, correlation, sum average, difference average, sum entropy, and difference entropy); and shape analysis with five features (compactness1, compactness2, elongation, flatness, and sphericity) were performed [32].

One radiologist drew volumes of interest (VOI) for each lesion using both manual corrections for automatic segmentation (semi-automatic segmentation) and without manual correction (fully automatic segmentation), twice per methods in four separate sessions (two semi-automatic and two fully automatic) at least 1 month apart to reduce memory recall and test intraobserver reproducibility.

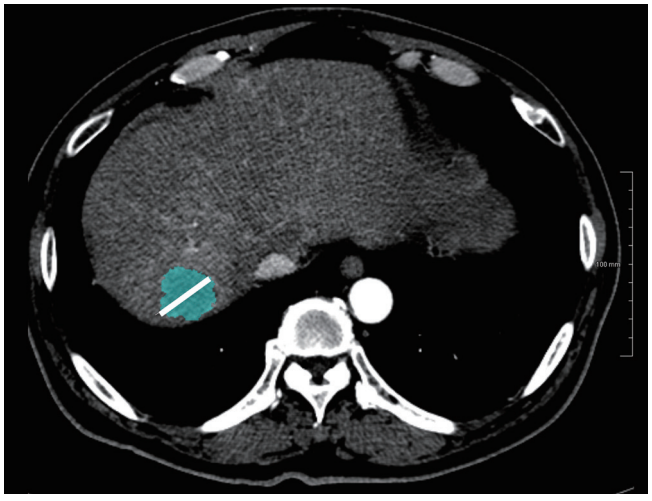

Fig. 2. Illustration of the application of the liver lesion segmentation tool. A 61-year-old male with cholangiocarcinoma. The reader manually draws a line (white line on the image) across the maximum dimension of the tumor. The software automatically segments the entire tumor volume.

Additionally, an ROI was drawn manually for the largest section once. To test interobserver reproducibility, 30 CT scans were randomly selected, and two sessions (one semi-automatic and one fully automatic) of segmentation, also with a 1-month interval, were performed by another radiologist (4 years of abdominal CT experience).

As Supplementary analysis (Supplementary Table 1), the arterial enhancement pattern of each tumor was visually assessed, performed by two radiologists.

Statistical Analysis

The time spent on segmentation and texture analysis was compared between the semi-automatic and fully automatic segmentation techniques using a paired *t* test. Reliability in obtaining the texture parameters between fully automatic and semi-automatic segmentation was assessed using intraclass correlation coefficient (ICC). Additionally, intraobserver and interobserver reproducibility was also assessed using ICC for each segmentation method. For comparison, the raw data from each segmentation session were used.

A univariable Cox proportional hazards regression was used to determine the relationship between the CT texture features and other clinicopathologic parameters and RFS. Multicollinearity was checked for pathologic size and other variables (semi-automatic diameter, semi-automatic volume, full-automatic diameter, full-automatic volume, ROI two-dimensional [2D] area, and ROI [2D] diameter). Variables with a variance inflation factor greater than 10 were removed from the multivariable analysis. Multivariable Cox proportional hazards regression were used to determine whether each clinicopathological or texture parameter, which was a significant factor in univariable analysis, was an independent prognostic factor for RFS. A p value of less than 0.05, indicated a statistical significance. All statistical analyses were performed using SPSS software (version 25; IBM Corp.) and MedCalc statistical software (version 19.0, MedCalc Software bvba).

RESULTS

Patients

Among the 89 patients included in this study, 58 (65.2%) patients had a recurrence and 31 (34.8%) patients had no recurrence until their final outpatient visit until December 2019. Other demographic, clinical, and pathological data are summarized in Table 1.

https://doi.org/10.3348/kjr.2021.0055

Korean Journal of Radiology
KJR

Table 1. Clinical and Pathologic Characteristics of 89 Study Patients

Characteristics	Data
Age, years	62.1 ± 8.3
Sex, male:female	64:25
Recurrence	
Yes	58 (65.2)
No	31 (34.8)
Tumor size, cm	5.8 ± 3.2
Histologic grade	
Well differentiated	17 (19.1)
Moderately differentiated	49 (55.1)
Poorly differentiated	23 (25.8)
Multiplicity	15 (16.9)
Extrahepatic extension	28 (31.5)
Vascular invasion	42 (47.2)
Regional lymph node metastasis	23 (25.8)
Underlying hepatitis	32 (36.0)
Laboratory finding	
CA 19-9, U/mL	3252.3 ± 11292.2
CEA, ng/mL	7.2 ± 16.5
AST, IU/L	36.7 ± 37.3
ALT, IU/L	40.4 ± 64.0
Total bilirubin, mg/dL	1.0 ± 1.1
Albumin, g/dL	4.1 ± 0.4

Data are mean ± standard deviation or number of patients with percentage in parentheses. ALT = alanine aminotransferase, AST = aspartate transaminase, CA 19-9 = carbohydrate antigen 19-9, CEA = cancer embryonic antigen

Table 2. Univariable Cox Regression Analysis of Clinicopathologic Parameters for Predicting RFS

Parameters	Hazard Ratio (95% CI)	*P*
Age (per year increase)	0.999 (0.968-1.031)	0.931
Sex (male to female)	0.810 (0.463–1.417)	0.460
Tumor size (per cm increase)	1.133 (1.059-1.213)	< 0.001
Histologic grade*	1.933 (0.263–14.200)	0.517
	1.941 (0.255–14.742)	0.522
Multiplicity	2.201 (1.159–4.180)	0.016
Extrahepatic extension	2.094 (1.236–3.548)	0.006
Vascular invasion	1.648 (0.980–2.771)	0.059
Regional lymph node metastasis	2.711 (1.547–4.751)	< 0.001
Underlying hepatitis	0.656 (0.375–1.147)	0.139
CA 19-9 (per U/mL increase)	1.000 (1.000–1.000)	0.321
CEA (per ng/mL increase)	1.021 (1.007–1.035)	0.003
AST (per IU/L increase)	1.004 (0.999–1.010)	0.153
ALT (per IU/L increase)	1.001 (0.998–1.005)	0.546
Bilirubin (per mg/dL increase)	1.071 (0.895–1.282)	0.455
Albumin (per g/dL increase)	0.656 (0.354–1.217)	0.181

*Histologic grade was compared between reference variable (well differentiated) and test variables (moderately differentiated, in the first raw and poorly differentiated, in the second raw). ALT = alanine aminotransferase, AST = aspartate transaminase, CA 19-9 = carbohydrate antigen 19-9, CEA = cancer embryonic antigen, CI = confidence interval, RFS = recurrence-free survival

Clinicopathological Parameters

The results of univariable Cox regression analysis regarding RFS for clinicopathologic parameters are described in Table 2. Among the clinicopathologic parameters, pathologic tumor size ($p < 0.001$), multiplicity ($p = 0.016$), extrahepatic extension ($p = 0.006$), regional lymph node metastasis ($p < 0.001$), and CEA ($p = 0.003$) were significant.

Texture Analysis Parameters

Time Spent on VOI Drawings

Reviewer 1 spent mean time ± standard deviation of 10 minutes and 48 seconds ± 13 minutes and 44 seconds for semi-automatic VOI segmentation per CTTA. Reviewer 2 used 9 minutes and 19 seconds ± 7 minutes and 59 seconds for semi-automatic VOI segmentation. In comparison, with fully automatic segmentation, reviewer 1 spent 1 minutes and 37 seconds ± 50 seconds per CTTA, and reviewer 2 spent 1 minutes and 23 seconds ± 37 seconds. The time spent on fully automatic tumor segmentation and CTTA was significantly shorter ($p < 0.001$) than that for semi-automatic segmentation by both reviewers. For manual ROI drawing, reviewer 1 spent 2 minutes and 1 seconds ± 1 minutes and 6 seconds.

Reliability between Semi-Automatic and Fully Automatic Segmentations

ICCs between semi-automatic and fully automatic segmentation ranged between 0.215–0.980 (Table 3). Among the first-order parameters, skewness and kurtosis were less reliable (< 0.5) compared to the other first-order parameters. The second-order parameters showed an ICC of 0.706–0.980, and shape features showed an ICC of 0.215–0.638 (Fig. 3). Among the 89 tumors, 34 (38.2%) had ill-defined margins. On the subgroup analysis (excluding tumors with ill-defined margins), improvement in the reproducibility was noted for shape features (0.515–0.792).

Reliability between Observers

Full results are provided in Supplementary Tables 2-5. The ICCs for intraobserver and interobserver reproducibility using fully automatic segmentation were 0.601–0.997 and 0.177–0.984, respectively (Supplementary Tables 3, 4).

https://doi.org/10.3348/kjr.2021.0055

Table 3. Reliability Between Parameters Extracted from Semi-Automatic Segmentation and Fully Automatic Segmentation

	All (n = 89)	Subgroup (n = 55)
Volume	0.971 (0.956–0.981)	0.982 (0.969–0.990)
Diameter	0.932 (0.896–0.955)	0.958 (0.928–0.976)
First-order		
Mean	0.967 (0.949–0.978)	0.958 (0.927–0.975)
Variance	0.744 (0.611–0.832)	0.786 (0.631–0.875)
Energy	0.899 (0.846–0.934)	0.904 (0.835–0.944)
Entropy	0.841 (0.758–0.895)	0.871 (0.779–0.925)
Skewness	0.407 (0.095–0.611)	0.446 (0.049–0.677)
Kurtosis	0.455 (0.171–0.641)	0.207 (-0.345–0.534)
Uniformity	0.827 (0.736–0.886)	0.874 (0.786–0.927)
Second-order		
GLCM IDM	0.980 (0.966–0.987)	0.987 (0.977–0.997)
GLCM contrast	0.967 (0.930–0.982)	0.966 (0.931–0.982)
GLCM correlation	0.706 (0.552–0.807)	0.756 (0.590–0.859)
GLCM sum average	0.715 (0.567–0.812)	0.529 (0.204–0.723)
GLCM diff average	0.978 (0.961–0.987)	0.983 (0.969–0.991)
GLCM sum entropy	0.828 (0.739–0.887)	0.864 (0.767–0.921)
GLCM diff entropy	0.960 (0.909–0.979)	0.968 (0.927–0.984)
Shape		
Compactness1	0.293 (-0.080–0.537)	0.520 (0.192–0.717)
Compactness2	0.215 (-0.201–0.486)	0.523 (0.197–0.718)
Elongation	0.562 (0.332–0.713)	0.775 (0.615–0.869)
Flatness	0.638 (0.449–0.762)	0.792 (0.614–0.884)
Sphericity	0.314 (-0.047–0.550)	0.515 (0.185–0.714)

Data are intraclass correlation coefficient values with 95% confidence interval in parentheses. Subgroup analysis was performed after excluding 34 tumors with ill-defined margins. diff = difference, GLCM = Gray-Level Co-occurrence Matrix, IDM = inverse difference moment

The ICCs between the two trials of semi-automatic VOI segmentation showed excellent reliability (> 0.8), except kurtosis (0.786) among the first-order texture parameters and compactness2 (0.777) among the shape parameters (Supplementary Table 2). The ICC between the two trials of fully automatic VOI segmentation showed excellent reliability (> 0.8) for all the first- and second-order texture parameters. However, shape features showed only a good reliability (0.601–0.812) (Supplementary Table 3).

Interobserver reproducibility was calculated for 30 randomly chosen tumors (Supplementary Table 4). Semi-automatic VOI segmentation showed excellent reproducibility between reviewers 1 and 2 (ICC > 0.8) for the first-and second-order parameters; however, less reproducibility (0.001–0.888) for the shape parameters. In contrast, fully automatic VOI segmentation, showed an ICC range of 0.684–0.984 except kurtosis among the first-order texture parameters, while less reproducibility (0.208–0.818) was observed for the shape parameters.

The results for the 55 subgroup of patients (also including 18 patients among them chosen for inter-observer analysis) after exclusion of patients with lesions with ill-defined margins are provided in Supplementary Tables 2, 3, and 5.

Association between Texture Parameters and RFS

Univariable Cox regression analysis for RFS using CT texture parameters with ROI drawings versus VOI drawings is summarized in Table 4. Univariable analysis of ROI drawings identified area (p = 0.001), diameter (p = 0.002), the first-order mean (p = 0.001), energy (p = 0.037), kurtosis (p = 0.037), and shape-flatness (p = 0.006) were significant. Univariable analysis of semi-automatic/fully automatic VOI segmentation revealed volume (p = 0.024/p = 0.010), diameter (p = 0.002/p = 0.004), and the first-order mean (p < 0.001/p = 0.001) were significant.

With multicollinearity analysis, semi-automatic volume, semi-automatic diameter, full-automatic volume, and ROI (2D) diameter were excluded from the multivariable analysis (Supplementary Table 6). The results of multivariable Cox regression analysis, including all clinicopathologic and texture parameters significant at univariable analyses, are shown in Table 5. For the ROI drawing method, extrahepatic extension (p = 0.017), regional lymph node metastasis (p = 0.010), CEA (p = 0.010), and area (p < 0.001) were significant predictors of RFS. For semi-automatic/fully automatic VOI segmentation, pathologic tumor size (p < 0.001/p < 0.001), regional lymph node metastasis (p = 0.030/

https://doi.org/10.3348/kjr.2021.0055

Korean Journal of Radiology
KJR

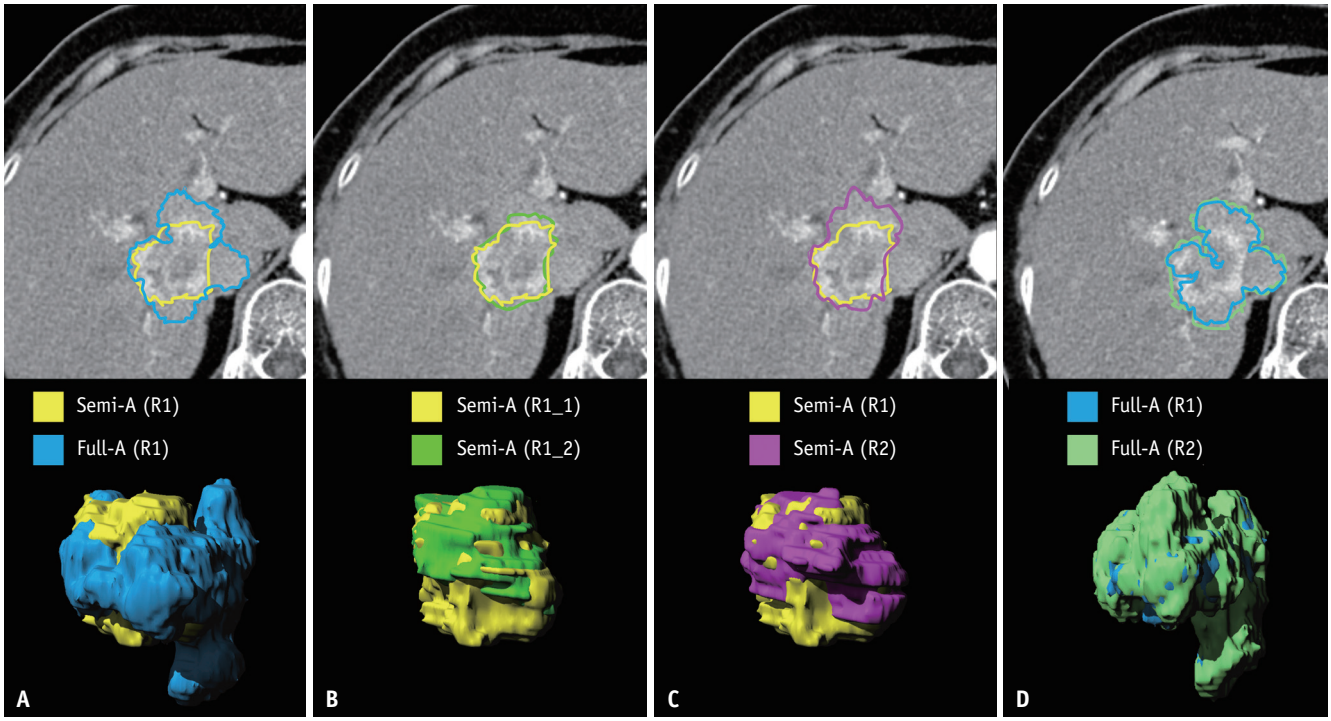

Fig. 3. Illustration of intraobserver and interobserver reproducibility of lesion segmentation. A 66-year-old female with cholangiocarcinoma showing arterial phase hyperenhancement, who did not show recurrence during 83.8 months follow-up after surgical resection.
A. Yellow is representative of semi-automatic segmentation and blue is representative of fully automatic segmentation, by radiologist 1. **B.** Light green is representative of the second trial of semi-automatic segmentation by radiologist 1. **C.** Purple is representative of semi-automatic segmentation by another radiologist, radiologist 2. **D.** Green is representative of fully automatic segmentation by radiologist 2.

p = 0.014), and the first-order mean (p = 0.006/p = 0.010) were significant factors for the prediction of RFS (Fig. 4).

DISCUSSION

Our study attempted to assess whether volumetric texture analysis of IMCCs using the fully automatic tumor segmentation technique can help predict RFS in patients undergoing surgical resection. In a comparison between the semi-automatic and fully automatic segmentation methods, we found that there was an excellent reliability between them in the first-and second-order parameters, except for skewness and kurtosis, while the time spent on fully automatic segmentation was dramatically and significantly shortened compared to semi-automatic segmentation. As for shape parameters that showed poor agreement, separate subgroup analysis performed after excluding tumors with ill-defined margins showed significant improvement in reliability. Finally, and in response to our original question, our study demonstrated that the first-order mean texture analysis was an independent predictor of RFS in patients with IMCCs using both semi-automatic and fully automatic segmentation methods, demonstrating that automatic segmentation can indeed be used as a prognostic tool.

The main obstacles in the clinical adoption of texture analysis are its reproducibility and generalizability [33]. Moreover, variability in tumor delineation can greatly influence radiomics analysis, and tumors with less sharp borders will accordingly have lower interobserver agreements [34]. Our study results in this regard are similar to the results of previous studies dealing with the segmentation of hepatic tumors [35,36] evaluating one or several parameters (attenuation on CT or analog-to-digital converters and enhancement degree on MRI). In those studies, semi-automatic VOI measurements showed better intraobserver and/or interobserver reproducibility than manual ROI measurements, while manual volume segmentation was shown to be tedious and time-consuming [27]. Our study results show that fully automatic VOI segmentation can demonstrate the same prognostic parameter as semi-automatic VOI segmentation; however, in a dramatically shorter time. Therefore, volumetric CTTA using fully automatic tumor segmentation can be utilized as a time-saving clinical tool that can

https://doi.org/10.3348/kjr.2021.0055

Table 4. Univariable Cox Regression Analysis of Texture Parameters for Predicting RFS

	Semi-Automatic		Fully Automatic		ROI Method	
	HR (95% CI)	*P*	HR (95% CI)	*P*	HR (95% CI)	*P*
Area/volume	1.001 (1.000–1.002)	0.024	1.001 (1.000–1.002)	0.010	1.045 (1.019–1.073)	0.001
Diameter	1.011 (1.004–1.018)	0.002	1.009 (1.003–1.016)	0.004	1.012 (1.004–1.019)	0.002
First-order						
Mean	0.972 (0.958–0.986)	< 0.001	0.977 (0.965–0.990)	0.001	0.976 (0.963–0.990)	0.001
Variance	1.000 (0.999–1.001)	0.836	0.999 (0.998–1.000)	0.291	1.000 (0.999–1.001)	0.609
Energy	1.000 (1.000–1.000)	0.493	1.000 (1.000–1.000)	0.064	1.000 (1.000–1.000)	0.037
Entropy	0.706 (0.320–1.562)	0.391	0.602 (0.266–1.360)	0.222	0.730 (0.341–1.560)	0.417
Skewness	1.355 (0.774–2.372)	0.288	0.725 (0.516–1.019)	0.064	2.289 (0.866–6.047)	0.095
Kurtosis	1.007 (0.968–1.048)	0.727	1.000 (0.963–1.039)	0.987	1.467 (1.024–2.102)	0.037
Uniformity	7.556 (0.298–191.561)	0.220	10.655 (0.344–330.459)	0.177	7.032 (0.319–155.088)	0.217
Second-order						
GLCM IDM	37.939 (0.254–5569.166)	0.155	54.332 (0.312–9467.910)	0.129	16.569 (0.192–1432.715)	0.217
GLCM contrast	0.603 (0.219–1.659)	0.328	0.583 (0.222–1.534)	0.275	0.716 (0.325–1.575)	0.406
GLCM correlation	1.030 (0.168–6.330)	0.975	0.553 (0.096–3.194)	0.508	1.220 (0.252–5.892)	0.805
GLCM sum average	1.022 (0.990–1.054)	0.184	1.014 (0.998–1.041)	0.282	1.030 (0.893–1.188)	0.687
GLCM diff average	0.264 (0.035–2.017)	0.199	0.233 (0.030–1.822)	0.165	0.377 (0.066–2.145)	0.272
GLCM sum entropy	0.714 (0.367–1.391)	0.323	0.632 (0.315–1.268)	0.196	0.781 (0.406–1.501)	0.458
GLCM diff entropy	0.344 (0.070–1.690)	0.189	0.290 (0.056–1.507)	0.141	0.468 (0.113–1.937)	0.295
Shape						
Compactness1	0.000 (0.000–48190.159)	0.102	0.000 (0.000–1.342 x 10^{17})	0.603	0.000 (0.000–1072388.411)	0.169
Compactness2	0.035 (0.001–1.969)	0.103	0.708 (0.031–15.939)	0.828	0.138 (0.002–8.097)	0.340
Elongation	1.776 (0.194–16.276)	0.611	1.758 (0.200–15.432)	0.611	0.561 (0.118–2.672)	0.468
Flatness*	1.735 (0.244–12.337)	0.582	0.354 (0.051–2.457)	0.294	21.861 (2.423–197.203)	0.006
Sphericity	0.039 (0.001–1.931)	0.103	0.372 (0.015–9.246)	0.546	0.160 (0.015–1.669)	0.125

CI = confidence interval, diff = difference, GLCM = Gray-Level Co-occurrence Matrix, HR = hazard ratio, IDM = inverse difference moment, RFS = recurrence-free survival

Table 5. Multivariable Cox Regression Analysis of Clinicopathologic and Texture Parameters for Predicting RFS

	Semi-Automatic		Fully Automatic		ROI Method	
	HR (95% CI)	*P*	HR (95% CI)	*P*	HR (95% CI)	*P*
Clinicopathologic						
Size*	1.166 (1.084–1.255)	< 0.001	1.171 (1.086–1.263)	< 0.001		0.089
Multiplicity		0.298		0.248		0.154
Extrahepatic extension		0.059		0.075	1.974 (1.127–3.457)	0.017
Regional LN metastasis	2.019 (1.069–3.812)	0.030	2.193 (1.169–4.112)	0.014	2.193 (1.203–3.997)	0.010
CEA		0.288		0.214	1.019 (1.005–1.034)	0.010
Texture analysis						
Area					1.053 (1.025–1.082)	< 0.001
Diameter				0.640		
First-order parameter						
Mean	0.980 (0.965–0.994)	0.006	0.982 (0.968–0.996)	0.010		0.140
Energy						0.661
Kurtosis						0.696
Shape						
Flatness						0.322

CEA = cancer embryonic antigen, CI = confidence interval, HR = hazard ratio, LN = lymph node, RFS = recurrence-free survival

https://doi.org/10.3348/kjr.2021.0055

Korean Journal of Radiology
KJR

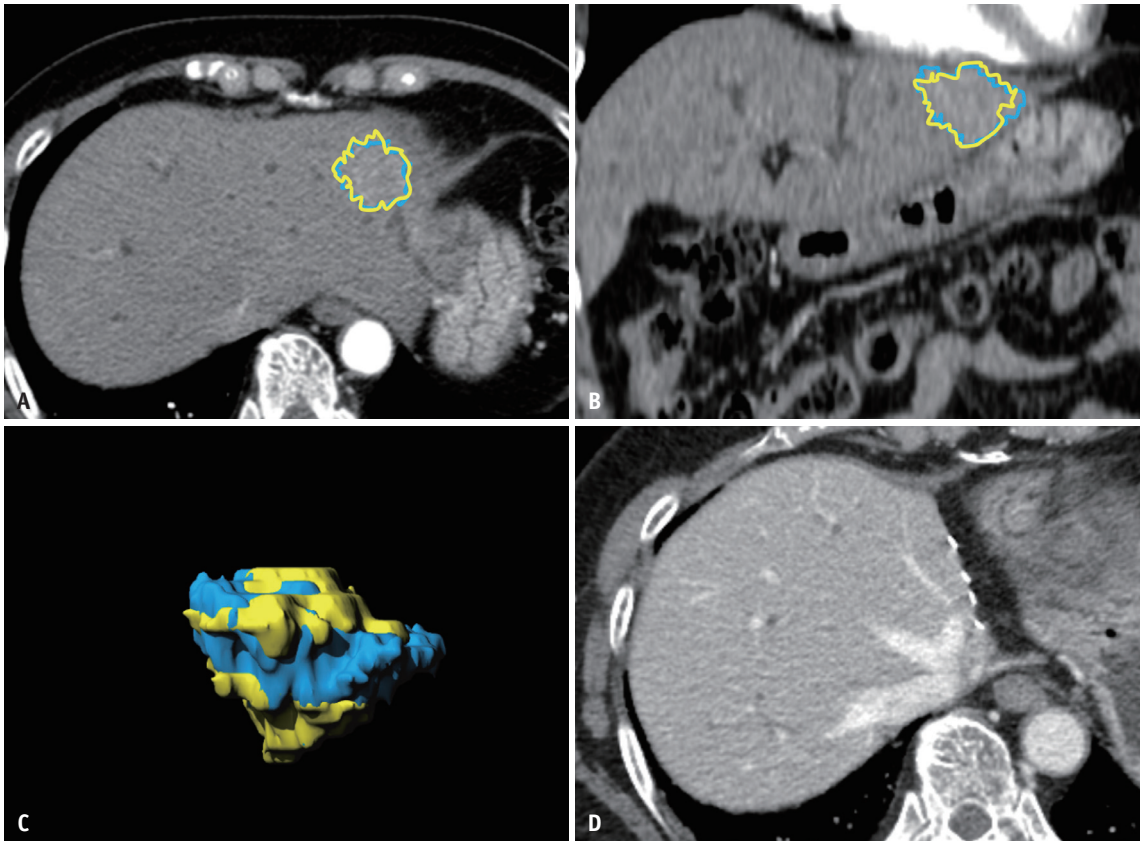

Fig. 4. Representative case of texture analysis predicting recurrence-free survival. A 64-year-old female with cholangiocarcinoma showing arterial phase isoenhancement and slight hyperenhancement.
A. Axial CT image. **B.** Coronal CT image. **C.** Volumetric reconstruction. The blue area is representative of fully automatic segmentation and the yellow area is representative of semi-automatic segmentation. The mean value of texture analysis was 89.1 and 85.8 on fully automatic segmentation and semi-automatic segmentation, respectively. The mean attenuation of 89 intrahepatic mass-forming cholangiocarcinomas was 64.6–66.3 (Supplementary Table 2, 3). **D.** No recurrence was observed for 77.8 months after surgical resection.

provide reproducible VOI drawings, and we suspect that semi-automatic or fully automatic segmentation will be the path forward [37] for wider acceptance of texture analysis in clinical studies.

In our comparison of the semi-automatic and fully automatic liver lesion segmentation techniques, we found that the reproducibility of both methods was overall good to excellent (ICC of 0.786–0.994 with semi-automatic segmentation and 0.932–0.997 with fully automatic segmentation) regarding the first-order histogram analysis and GLCM of the second-order analysis, which is comparable to the reproducibilities reported in other recent studies [38,39]. However, shape features extracted from fully automatic VOI segmentation demonstrated inferior reproducibility (0.601–0.812) compared to that of semi-automatic VOI segmentation (0.777–0.899). This lower reproducibility of shape features may have resulted from the inherent limitation of the auto-segmentation mechanism used in this study, as computations can easily be affected by even minute differences in the pathway of line strokes [30,31]. However, even the interobserver reproducibility of the semi-automatic VOI segmentation method between the two radiologists was poor (0.001–0.888), highlighting the difficulty in reproducing similar measurements. Thus, considering that cholangiocarcinoma has ill-defined margins, we performed a separate subgroup analysis, excluding tumors with ill-defined margins. According to the results of this analysis, the interobserver reproducibility between fully automatic VOI segmentation showed greater improvement than that of semi-automatic VOI segmentation. Therefore, we believe that fully automatic VOI segmentation would be acceptable for the volumetric CTTA of most IMCC cases, except for highly infiltrative tumors.

Finally, our study demonstrated that the first-order mean parameter of VOI CTTA on AP images was a favorable predictor of RFS in patients with IMCC, which is in good agreement with previous studies [9-11], which reported that IMCCs with arterial enhancement showed better

 https://doi.org/10.3348/kjr.2021.0055

prognosis than IMCCs without arterial enhancement. However, in previous studies [9-11], visual inspection was used to determine the pattern of enhancement by comparing the enhancement of the tumor with that of the background liver parenchyma qualitatively using binary or tertiary classification (hyperenhancement totally or partially, or hypoehancement). We also performed ROI attenuation measurements for the largest tumor section at the arterial phase in this study; however, the first-order mean was not demonstrated to be a significant factor in the multivariable analysis. This may suggest that VOI drawing may be more representative of the whole tumor than 2D ROI drawing. The growing evidence that the arterial enhancement pattern and degree of IMCC are related to the prognosis of IMCC also correlates well with the currently developing histologic concepts of cholangiocarcinoma. According to recent immunohistochemical staining studies [40,41], IMCCs can be divided into large and small duct types. Small duct type IMCCs frequently show a larger area of arterial phase hyperenhancement on CT or MRI due to the reflection of its nonschirrhous nature and has a more favorable survival probability than the large duct type [40-42]. Although the pathologic database from our hospital did not provide specific information regarding the origin of the cell type, our study may provide a radiologic-histologic correlation of IMCCs. Although many validation studies are warranted, quantitative texture analysis of arterial phase hyperenhancement of IMCCs may be an option for future prognostic markers of IMCCs. However, the limited number of significant prognostic variables from our texture analysis result doubts the added clinical value of texture analysis for predicting the RFS of IMCC. Nevertheless, objective numeric data from our texture analysis support previous articles [9-11] based on subjective visual analysis, with more statistical power (Supplementary Table 1). In addition, the application of fully automatic segmentation tools will help to utilize image characteristics of tumors, not only for radiologists but also for clinicians not familiar with image interpretation, with shorter time spent.

There are several limitations to our study that should be mentioned. First, owing to its retrospective nature, various CT machines were used in our study, although only FBP reconstructed images taken at 120 kVp were chosen to lower interscanner variance. However, the use of different CT machines may lead to better generalizability. Second, we did not analyze all the second-order features of the texture analysis provided in the texture analysis program. Specifically, Gray Level Run Length Matrix (GLRLM) and Gray Level Size Zone Matrix (GLSZM) were not analyzed, and filters were not applied. Thus, further studies are warranted to validate the reproducibility of the entirety of features in PyRadiomics. Lastly, our decision to include only patients who underwent surgery may have introduced a selection bias. Therefore, the extent of extrapolation of our study results could be limited to patients with surgically resectable IMCCs.

In conclusion, our study results demonstrated that volumetric CTTA of arterial phase images using the fully automatic segmentation approach could be used as a biological prognostic tool in patients with IMCC, with comparable reproducibility of semi-automatic CTTA, in far less time, thereby potentially resolving one of the major technical challenges of texture analysis.

Supplement

The Supplement is available with this article at https://doi.org/10.3348/kjr.2021.0055.

Conflicts of Interest

Jeong Min Lee. Activities related to the present article: disclosed no relevant relationships. Activities not related to the present article: is a consultant to Samsung Medison; institution received grants from Samsung Medison, GE Healthcare, Philips Healthcare, Bayer, Guerbet, Bracco, Central Medical Service, and Canon Healthcare; institution was compensated for lectures by Bayer, Samsung Medison, and Bracco. Other authors declare that they have no conflict of interest.

Author Contributions

Conceptualization: Jeong Min Lee, Sungeun Park. Data curation: Sungeun Park. Formal analysis: Sungeun Park. Investigation: Sungeun Park. Methodology: Sungeun Park, Ijin Joo. Project administration: Jeong Min Lee, Sungeun Park. Resources: Jeong Min Lee. Software: Sungeun Park. Supervision: Jeong Min Lee. Validation: Sungeun Park, Jihyuk Lee, Junghoan Park, Jae Seok Bae, Jae Hyun Kim. Visualization: Sungeun Park. Writing—original draft: Sungeun Park. Writing—review & editing: Ijin Joo, Jeong Min Lee.

ORCID iDs

Sungeun Park
https://orcid.org/0000-0003-1462-9689

Korean Journal of Radiology
KJR

Jeong Min Lee
https://orcid.org/0000-0003-0561-8777
Junghoan Park
https://orcid.org/0000-0002-0636-3756
Jihyuk Lee
https://orcid.org/0000-0001-8208-2297
Jae Seok Bae
https://orcid.org/0000-0003-2768-7917
Jae Hyun Kim
https://orcid.org/0000-0002-6691-3932
Ijin Joo
https://orcid.org/0000-0002-1341-4072

REFERENCES

1. Sempoux C, Jibara G, Ward SC, Fan C, Qin L, Roayaie S, et al. Intrahepatic cholangiocarcinoma: new insights in pathology. *Semin Liver Dis* 2011;31:49-60
2. Zhang H, Yang T, Wu M, Shen F. Intrahepatic cholangiocarcinoma: epidemiology, risk factors, diagnosis and surgical management. *Cancer Lett* 2016;379:198-205
3. Dhanasekaran R, Hemming AW, Zendejas I, George T, Nelson DR, Soldevila-Pico C, et al. Treatment outcomes and prognostic factors of intrahepatic cholangiocarcinoma. *Oncol Rep* 2013;29:1259-1267
4. Mavros MN, Economopoulos KP, Alexiou VG, Pawlik TM. Treatment and prognosis for patients with intrahepatic cholangiocarcinoma: systematic review and meta-analysis. *JAMA Surg* 2014;149:565-574
5. Rizvi S, Gores GJ. Pathogenesis, diagnosis, and management of cholangiocarcinoma. *Gastroenterology* 2013;145:1215-1229
6. Gil E, Joh JW, Park HC, Yu JI, Jung SH, Kim JM. Predictors and patterns of recurrence after curative liver resection in intrahepatic cholangiocarcinoma, for application of postoperative radiotherapy: a retrospective study. *World J Surg Oncol* 2015;13:227
7. Murakami Y, Uemura K, Sudo T, Hashimoto Y, Nakashima A, Kondo N, et al. Prognostic factors after surgical resection for intrahepatic, hilar, and distal cholangiocarcinoma. *Ann Surg Oncol* 2011;18:651-658
8. Kiriyama M, Ebata T, Aoba T, Kaneoka Y, Arai T, Shimizu Y, et al. Prognostic impact of lymph node metastasis in distal cholangiocarcinoma. *Br J Surg* 2015;102:399-406
9. Ariizumi S, Kotera Y, Takahashi Y, Katagiri S, Chen IP, Ota T, et al. Mass-forming intrahepatic cholangiocarcinoma with marked enhancement on arterial-phase computed tomography reflects favorable surgical outcomes. *J Surg Oncol* 2011;104:130-139
10. Fujita N, Asayama Y, Nishie A, Ishigami K, Ushijima Y, Takayama Y, et al. Mass-forming intrahepatic cholangiocarcinoma: enhancement patterns in the arterial phase of dynamic hepatic CT - Correlation with clinicopathological findings. *Eur Radiol* 2017;27:498-506
11. Kim SA, Lee JM, Lee KB, Kim SH, Yoon SH, Han JK, et al. Intrahepatic mass-forming cholangiocarcinomas: enhancement patterns at multiphasic CT, with special emphasis on arterial enhancement pattern--correlation with clinicopathologic findings. *Radiology* 2011;260:148-157
12. Asayama Y, Yoshimitsu K, Irie H, Tajima T, Nishie A, Hirakawa M, et al. Delayed-phase dynamic CT enhancement as a prognostic factor for mass-forming intrahepatic cholangiocarcinoma. *Radiology* 2006;238:150-155
13. Gillies RJ, Kinahan PE, Hricak H. Radiomics: images are more than pictures, they are data. *Radiology* 2016;278:563-577
14. Lambin P, Leijenaar RTH, Deist TM, Peerlings J, de Jong EEC, van Timmeren J, et al. Radiomics: the bridge between medical imaging and personalized medicine. *Nat Rev Clin Oncol* 2017;14:749-762
15. Lubner MG, Smith AD, Sandrasegaran K, Sahani DV, Pickhardt PJ. CT texture analysis: definitions, applications, biologic correlates, and challenges. *Radiographics* 2017;37:1483-1503
16. Miles KA, Ganeshan B, Hayball MP. CT texture analysis using the filtration-histogram method: what do the measurements mean? *Cancer Imaging* 2013;13:400-406
17. Ng F, Ganeshan B, Kozarski R, Miles KA, Goh V. Assessment of primary colorectal cancer heterogeneity by using whole-tumor texture analysis: contrast-enhanced CT texture as a biomarker of 5-year survival. *Radiology* 2013;266:177-184
18. Ganeshan B, Skogen K, Pressney I, Coutroubis D, Miles K. Tumour heterogeneity in oesophageal cancer assessed by CT texture analysis: preliminary evidence of an association with tumour metabolism, stage, and survival. *Clin Radiol* 2012;67:157-164
19. Skogen K, Ganeshan B, Good C, Critchley G, Miles K. Measurements of heterogeneity in gliomas on computed tomography relationship to tumour grade. *J Neurooncol* 2013;111:213-219
20. Li M, Fu S, Zhu Y, Liu Z, Chen S, Lu L, et al. Computed tomography texture analysis to facilitate therapeutic decision making in hepatocellular carcinoma. *Oncotarget* 2016;7:13248-13259
21. Scalco E, Rizzo G. Texture analysis of medical images for radiotherapy applications. *Br J Radiol* 2017;90:20160642
22. Davnall F, Yip CS, Ljungqvist G, Selmi M, Ng F, Sanghera B, et al. Assessment of tumor heterogeneity: an emerging imaging tool for clinical practice? *Insights Imaging* 2012;3:573-589
23. Ganeshan B, Miles KA. Quantifying tumour heterogeneity with CT. *Cancer Imaging* 2013;13:140-149
24. Liang W, Xu L, Yang P, Zhang L, Wan D, Huang Q, et al. Novel nomogram for preoperative prediction of early recurrence in intrahepatic cholangiocarcinoma. *Front Oncol* 2018;8:360
25. Zwanenburg A, Vallières M, Abdalah MA, Aerts HJWL, Andrearczyk V, Apte A, et al. The image biomarker standardization initiative: standardized quantitative radiomics for high-throughput image-based phenotyping. *Radiology* 2020;295:328-338

 https://doi.org/10.3348/kjr.2021.0055

26. Kuhl CK, Truhn D. The long route to standardized radiomics: unraveling the knot from the end. *Radiology* 2020;295:339-341
27. Parmar C, Rios Velazquez E, Leijenaar R, Jermoumi M, Carvalho S, Mak RH, et al. Robust radiomics feature quantification using semiautomatic volumetric segmentation. *PLoS One* 2014;9:e102107
28. Chlebus G, Schenk A, Moltz JH, van Ginneken B, Hahn HK, Meine H. Automatic liver tumor segmentation in CT with fully convolutional neural networks and object-based postprocessing. *Sci Rep* 2018;8:15497
29. Li W. Automatic segmentation of liver tumor in CT images with deep convolutional neural networks. *J Comput Commun* 2015;3:146-151
30. Kuhnigk JM, Dicken V, Bornemann L, Bakai A, Wormanns D, Krass S, et al. Morphological segmentation and partial volume analysis for volumetry of solid pulmonary lesions in thoracic CT scans. *IEEE Trans Med Imaging* 2006;25:417-434
31. Moltz JH, Bornemann L, Kuhnigk JM, Dicken V, Peitgen E, Meier S, et al. Advanced segmentation techniques for lung nodules, liver metastases, and enlarged lymph nodes in CT scans. *IEEE J Sel Top Signal Process* 2009;3:122-134
32. Xie T, Wang Z, Zhao Q, Bai Q, Zhou X, Gu Y, et al. Machine learning-based analysis of MR multiparametric radiomics for the subtype classification of breast cancer. *Front Oncol* 2019;9:505
33. Park JE, Park SY, Kim HJ, Kim HS. Reproducibility and generalizability in radiomics modeling: possible strategies in radiologic and statistical perspectives. *Korean J Radiol* 2019;20:1124-1137
34. Pavic M, Bogowicz M, Würms X, Glatz S, Finazzi T, Riesterer O, et al. Influence of inter-observer delineation variability on radiomics stability in different tumor sites. *Acta Oncol* 2018;57:1070-1074
35. Chalian H, Tochetto SM, Töre HG, Rezai P, Yaghmai V. Hepatic tumors: region-of-interest versus volumetric analysis for quantification of attenuation at CT. *Radiology* 2012;262:853-861
36. Bonekamp D, Bonekamp S, Halappa VG, Geschwind JF, Eng J, Corona-Villalobos CP, et al. Interobserver agreement of semi-automated and manual measurements of functional MRI metrics of treatment response in hepatocellular carcinoma. *Eur J Radiol* 2014;83:487-496
37. Varghese BA, Cen SY, Hwang DH, Duddalwar VA. Texture analysis of imaging: what radiologists need to know. *AJR Am J Roentgenol* 2019;212:520-528
38. Yap FY, Hwang DH, Cen SY, Varghese BA, Desai B, Quinn BD, et al. Quantitative contour analysis as an image-based discriminator between benign and malignant renal tumors. *Urology* 2018;114:121-127
39. Verhaart RF, Fortunati V, Verduijn GM, van Walsum T, Veenland JF, Paulides MM. CT-based patient modeling for head and neck hyperthermia treatment planning: manual versus automatic normal-tissue-segmentation. *Radiother Oncol* 2014;111:158-163
40. Joo I, Lee JM, Yoon JH. Imaging diagnosis of intrahepatic and perihilar cholangiocarcinoma: recent advances and challenges. *Radiology* 2018;288:7-13
41. Nakanuma Y, Sato Y, Harada K, Sasaki M, Xu J, Ikeda H. Pathological classification of intrahepatic cholangiocarcinoma based on a new concept. *World J Hepatol* 2010;2:419-427
42. Nam JG, Lee JM, Joo I, Ahn SJ, Park JY, Lee KB, et al. Intrahepatic mass-forming cholangiocarcinoma: relationship between computed tomography characteristics and histological subtypes. *J Comput Assist Tomogr* 2018;42:340-349

https://doi.org/10.3348/kjr.2021.0055